The protective effects of wine pomace products on the vascular endothelial barrier function

Gisela Gerardi, Mónica Cavia-Saiz*, María D. Rivero-Pérez, María L. González-SanJosé and Pilar Muñiz

Department of Biotechnology and Food Science, Faculty of Sciences, University of Burgos, Plaza Misael Bañuelos, 09001, Burgos, Spain.

***Corresponding author**: Dra. Mónica Cavia Saiz, Plaza Misael Bañuelos, Facultad de Ciencias, Departamento de Biotecnología y Ciencia de los Alimentos, 09001, Burgos, Spain.

E-mail: monicacs@ubu.es

Phone: +34-947258800 Ext. 8210

Fax: +34-947258831

Email addresses: Gisela Gerardi (mggerardi@ubu.es), Mónica Cavia-Saiz (monicacs@ubu.es), María D. Rivero-Pérez (drivero@ubu.es), María L. González-SanJosé (marglez@ubu.es), Pilar Muñiz (pmuniz@ubu.es).

ORCID iDs:

Gisela Gerardi https://orcid.org/0000-0003-2510-0422

Mónica Cavia-Saiz https://orcid.org/0000-0001-5132-381X

María D. Rivero-Pérez https://orcid.org/0000-0003-0907-4009

María L. González-SanJosé https://orcid.org/0000-0003-2973-7287

Pilar Muñiz https://orcid.org/0000-0002-9306-0082

Abstract

Endothelial dysfunction is associated with cardiovascular diseases and involves a chronic inflammatory process that together with oxidative stress increase the permeability of the vascular endothelium. The aim of this study was to evaluate the role of red and white wine pomace products (rWPP and wWPP) in the preservation of the endothelial integrity in hyperglycemia of EA.hy926 endothelial cells. EA.hy926 endothelial cells exposed to hyperglycemia were treated with the *in vitro* digested fractions of the rWPP and wWPP. A Real Time Cellular Analysis (RTCA) system was performed to evaluate the endothelial monolayer integrity after INF-γ stimulation of the pre-treated endothelial cells with the digested fractions. Changes in cell viability, NO, ROS and NOX4 were recorder and actin cytoskeleton and E-cadherin junctions were evaluated by immunofluorescence. All digested fractions prevent the hyperglycemic actions in the cell viability and NO/ROS balance. The inflammatory mediator INF-γ and hyperglycemia caused a decrease in RTCA adhesion of EA.hy926 endothelial cells monolayer. Pre-treatment with all digested fractions enhanced EA.hy926 endothelial monolayer integrity and preserved actin cytoskeleton and E-cadherin junctions. These *in vitro* studies elucidate that the anti-hyperglycemic and anti-inflammatory actions of wine pomace products involve the decrease of ROS production and the stabilization of junction proteins via modulation of VE-cadherin and actin cytoskeleton suggesting a potential prevention of the endothelial damage by these natural products.

Keywords: polyphenols, endothelial cells, hyperglycemic, gamma interferon, E-cadherin, xCELLigence, wine pomace.

52

53

54 **1 Introduction**

55 Endothelial dysfunction, associated with a large number of cardiovascular risk factors, is a
56 precursor of atherosclerosis and other cardiovascular diseases [1]. Endothelial hyperpermeability is
57 one of the initial responses of endothelial cells to certain types of diseases such as hyperglycemia
58 and hyperlipidemia [2]. Changes in the barrier function can exacerbate tissue damage throughout
59 disease progression. Thus, normal vasculature recovery will imply a reduction of this
60 hyperpermeable state, which might also contribute to a reduced risk of cardiovascular disease.
61 Dynamic opening and closing of endothelial junctions and their regulation is essential for the
62 maintenance of vascular integrity. Intercellular adhesion within the endothelium is mainly
63 dependent on adherens junctions, composed of cell-cell adhesion proteins such as VE-cadherin [3].
64 Moreover, these adhesion molecules, transfer intracellular signals that modulate contact inhibition
65 of cell growth, cell polarity, and lumen formation, among others [4].

66 Hyperglycemia in endothelial cells promotes oxidative stress, mainly generated by the enzyme
67 NADPH oxidase 4 (NOX4) [5]. The production of reactive oxygen species (ROS) depends on the
68 level of expression of NOX4 and the phosphorylation of its units. The regulation of NOX4
69 expression could reduce endothelial ROS production and it plays an important role in the
70 reduction of endothelial hyperpermeability associated with hyperglycemia. Moreover,
71 hyperglycemia activates nuclear factor-kappa B (NF-κB) in endothelial cells, and thus activates
72 the transcription of pro-inflammatory genes including TNF-α, IL-1, IL-8 [6].

73 Increased vascular permeability, cell adhesion molecule (CAM) up-regulation, ROS formation,
74 and NF-κB activation were observed in high-glucose-induced vascular inflammation of
75 EA.hy926 endothelial cells and mouse models [7,8]. Furthermore, ROS generation leads to VE-
76 cadherin endocytosis and increased vascular permeability [3]. Therefore, high levels of ROS and
77 pro-inflammatory cytokines play a central role in the initiation and progression of endothelial
78 barrier dysregulation. These considerations suggest that antioxidant and anti-inflammatory

79 compounds could be used in the maintenance of endothelial integrity [9–13]. Polyphenolic wine
80 pomace compounds include flavonoids (anthocyanins, flavan-3-ols, flavonols) and non-
81 flavonoids (phenolic acids, stilbenes), with well-established antioxidant and the anti-
82 inflammatory effects [14,15]. Indeed, recent studies from our laboratory have demonstrated that
83 wine-pomace polyphenols provide effective protection against endothelial dysfunction, increase
84 the bioactivity of nitric oxide, ameliorate oxidative stress, and modulate various signaling
85 pathways [16–18].
86 Based on the consideration that wine pomace products contribute to preventing oxidative stress
87 and the subsequent protection of endothelial damage [15], we hypothesized that the antioxidant
88 properties of the wine pomace products, extracted from both red and white grape skins, can
89 attenuate the deleterious effects of hyperglycemic and inflammatory conditions on endothelial
90 permeability. The results of this study would contribute to the understanding of cell-cell junction
91 regulation, introducing a new function of wine pomace polyphenols as a stabilizer of endothelial
92 integrity.
93
94 **2 Materials and methods**
95 **2.1 Wine pomace products (WPPs)**
96 The powdered products examined in this study was prepared at the University of Burgos
97 according to a previously described method [19]. The products were obtained from seedless red and
98 white wine pomace (rWPP and wWPP, respectively) using a heat treatment as stabilisation
99 process, and their main characteristics and composition (dietary fibre, fat, protein, minerals and
100 phenolic classes) have been previously described [20] and are summarized in Table 1 and Table 2
101 of supporting information. *In vitro* digestion of the rWPP and wWPP was performing as we
102 describe in a previous study [15]. This procedure mainly involved two sequential phases that
103 simulate conditions along the gut: enzymatic gastrointestinal digestion and colonic fermentation.
104 Briefly, the wine pomaces (rWPP and wWPP) were incubated with pepsin (100.000 U/g, pH 2,
105 40ºC 1h), pancreatin (16.7 mg/g, pH 7.5, 37ºC 6h), lipase (10.000 U/g, pH 7.5, 37ºC 6h), bile

106 salts (17 mg/g, pH 7.5, 37ºC 6h), α-amilase (8.800 U/g, pH 7, 37ºC 16h), and amyloglucosidase
107 (10 U/g, pH 7, 37ºC 1h) and then the samples were centrifuged at 3000 g during 15 minutes at
108 25ºC. The supernatants were transferred into cellulose membrane dialysis tubing and dialyzed
109 against Milli-Q water for 24 h. The dialysates were collected, lyophilized, weighed, and stored at
110 -20ºC. This fraction was labelled as "Wine Pomace potentially bioavailable fraction after Gastro-
111 intestinal digestion: WPGI". The dialysis step was performed to model the passive absorption of
112 the intestinal barrier and obtain potentially bioavailable fractions. Then, the dialysis retentate and
113 the residue from the centrifugation step were mixed and then subjected to an *in vitro* colonic
114 fermentation. The microbial colonic inoculum was obtained by mixing the caecal content from 5
115 male Wistar rats. All procedures with these animals were performed following the guidelines
116 established by the Ethics Committee of both the University Hospital of Burgos and the University
117 of Burgos. The samples were incubated with the inoculum (2 g caecal content/g sample) 24 h at
118 37ºC in anaerobic conditions. Then, the resultant colonic fermented fractions were separated by
119 centrifugation at 2500g during 10 minutes at 25ºC. The supernatants were transferred into
120 cellulose membrane dialysis tubing and dialyzed against Milli-Q water for 24 h. The dialysates
121 obtained were named "Wine Pomace potentially bioavailable fraction after colonic Fermentation:
122 WPF". Three replicates were carried out for each fraction. Negative digested controls (without
123 WPPs) for both types of fractions were also prepared.

124 **2.2 HPLC phenolic compounds analysis**

125 The digested fractions (10 mg/ml, water solution) were analyzed according to a slightly modified
126 version of a method described before [21]. Identification and quantification of stilbenes, flavan-3-
127 ols and flavonols was carried out using analytical reversed-phase HPLC on an Agilent 1100 series
128 HPLC system (Agilent Technologies Inc., Palo Alto, CA, USA) coupled to a diode array detector
129 and a Spherisorb3® ODS2 reversed phase C18 column (250 mm x 4.6 mm, 3 µm particle size;
130 Waters Cromatografia S.A., Barcelona, Spain). Samples were injected in duplicate, and
131 calibration was performed by injecting the standards three times at five different concentrations.

132 Peak identification was performed by comparison of retention times and diode array spectral
133 characteristics with the standards. The results were expressed in μg/g.

134 **2.3 GC-MS/MS phenolic acids analysis**

135 Concentration of phenolic acids were measured in each digested fraction by using a gas
136 chromatography coupled to electron ionization mass spectrometry (GC-MS/MS) following a
137 method previously described [22], with slight modifications. 1 mg of the digested fractions were
138 derivatized with 50 μL of BSTFA and 50 μL of dry pyridine, mixed and heated at 40 °C for 30
139 min. The trimethylsilyl (TMS) derivatives obtained were analyzed on an Agilent 7890B GC
140 System (Agilent Technologies, Inc., Palo Alto, CA) coupled to an Agilent 7010 GC/MS
141 TripleQuad detector and fitted with an DB5-MS column (25 m x 0.20 mm, 0.33 μm film thickness,
142 Agilent Technologies) using helium as the carrier gas with an inlet pressure of 30 kPa. Injections
143 were made in the split-less mode. For quantification, calibration curves were established by
144 measuring peak areas versus response in comparison with the internal standard over a range of
145 each analyte concentrations. The concentration of phenolic acids in plasma was finally expressed
146 as μg phenolic acid/g of digested fraction.

147 **2.4 Cell culture and treatment**

148 The immortalized cell line EA.hy926 was kindly provided by Dr. Diana Hernández-Romero from
149 the research group 'Arterial thrombosis and interstitial, vascular and myocardial remodelling'
150 (IMIB-Arrixaca/University of Murcia, Murcia, Spain). The concentration of the WPGI and the
151 WPF digested fractions used 2.5 μg GAE/ml as their final concentration in the cell medium. This
152 dose of 14.7 μM was selected according to previous studies of bioavailability in humans [23] and
153 Wistar rats [24] that have shown that after intake of 500 mg of polyphenols or 50-300 mg/kg BW of
154 WPP, the concentration of total phenolic metabolites in plasma may reach about 5-50 μM. Cells
155 were maintained in DMEM 5.6 mM of Glucose supplemented with 10% FBS, 1% P/S, and 1%
156 L-glutamine solution at 37 °C in a humidified incubator with 5% CO2. The medium during the
157 treatment incubation period was DMEM, either 5.6 (normoglycemia) or 25 mM (hyperglycemia)
158 Glucose, supplemented with 1% FBS, 1% P/S, 1% L-glutamine solution, and 0.1% DMSO.

159 **2.5 Cell viability assessment**

160 Cell viability was analysed using the MTT method [25]. The results were expressed as % cell
161 viability with respect to control cells grown in the normoglycemic medium.

162 **2.6 Real-Time Cell Proliferation Assay**

163 Cell proliferation was monitored in real-time using the xCELLigence Real-Time Cellular
164 Analysis (RTCA) system (Roche, Germany). The instrument measures the electrical resistance of
165 the sensor electrodes that is proportional to the number of cells attached to the sensors, which
166 allows real time measurements by probing cell growth at different time intervals. The electrical
167 impedance value of each well was automatically monitored by the xCELLigence system and
168 expressed as a cell index (CI) value. Briefly, background measurements were took after adding
169 100 µL of the appropriate medium to the wells of the L8 E-plate. Cell suspension (5 × 104
170 cells/well) was added to the wells. The attachment and proliferation of the cells were monitored
171 every 5 minutes using RTCA system. Approximately 24 hours after seeding, when the cells are
172 in the log growth phase, the cells were treated with WPGI and WPF (2.5 µg GAE/ml) and
173 continuously monitored for up to 96 hours. The cells were also treated with medium alone, which
174 served as vehicle control.

175 **2.7 Real-Time Cell Permeability Assay**

176 *In vitro* cell permeability was assessed in xCELLigence Real-Time Cellular Analysis (RTCA)
177 system (Roche, Germany). EA.hy926 endothelial cells were seeded on L8 E-Plates (Roche
178 Applied Science) at a density of 10000 cells/well and allow reaching confluence. Then EA.hy926
179 endothelial cells were treated with 2.5 µg GAE/ml of WPGI and WPF fractions for 4 hours prior
180 to INF-γ treatment (3000 U/ml). Changes on the impedance were monitored every 5 minutes
181 using RTCA system and continuously monitored for up to 72 hours. The cells were also treated
182 with medium alone, which served as vehicle control and with gamma interferon, which served as
183 permeability altered control. Cell sensor impedance was expressed as an arbitrary unit called Cell
184 Index. The plot shows data normalized to the last time point before INF-γ addition, and curves
185 were plotted with control wells set as baseline.

186 **2.8 Immunofluorescence assays**

187 EA.hy926 endothelial cells were seeded at a density of 120000 cells/well in six-wells multidiches
188 containing glass coverslips and allow to reach confluence. Then EA.hy926 endothelial cells were
189 treated with 2.5 µg GAE/ml of WPGI and WPF fractions for 4 hours prior to 1.5 hours INF-γ
190 treatment (3000 U/ml). After fixing the cells with 4% p-formaldehyde, the cells were
191 permeabilized with 0.05% Triton X-100 and incubated with the corresponding staining:
192 CytoPainter Phalloidin iFluor 488 Reagent (Abcam) and Rb mAb to E-cadherin [EP7004] Alexa
193 Fluor 594 (Abcam). Then the cells were mounted with Fluoroshield mounting medium (Abcam).
194 The cells were also treated with medium alone, which served as vehicle control and with gamma
195 interferon, which served as permeability altered control. Images were taken with a Leica TCS
196 SP5 Confocal Laser Scanning Microscope and LAS AF Software (Leica Microsystems, Wetzlar,
197 Germany). The image analysis was realized with ImageJ Software.

198 **2.9 NO and ROS determinations**

199 EA.hy926 endothelial cells were seeded on T-25 flask at a density of 125000 cells/ml for NO
200 determination or 96-multiwell plates at a density of 20000 cells/well for ROS measurement and
201 allow them reaching confluence. When the cells are in the log growth phase, they were treated
202 with WPGI and WPF (2.5 µg GAE/ml) and with or without INF-γ (3000 U/ml) before NO and
203 ROS measurements. Then, total extracellular nitrite and nitrate was determined in the cell medium
204 using the Cayman's Nitrate/Nitrite Colorimetric Assay kit (Cayman Chemical, Ann Arbor, MI,
205 USA) according to the supplier's instructions. The % viability determined by the MTT assays run
206 in parallel was used to normalize cellular production of NO, which was finally expressed as µM
207 of nitrite or nitrate. Overall intracellular ROS production in EA.hy926 endothelial cells was
208 measured by the 2′,7′-dichlorofluorescein (DCF) assay [26], with certain modifications as we
209 describe in a previous study [15].

210 **2.10 Quantitative Real Time PCR (q-PCR) analysis**

211 q-PCR was performed as previously described [15]. Briefly, EA.hy926 endothelial cells were seeded
212 on T-25 flask at a density of 20000 cells/well and when the cells are in the log growth phase, the

213 cells were treated with WPGI and WPF (2.5 µg GAE/ml) and with or without INF-γ (3000 U/ml).
214 Then, cells were trypsinized, centrifuged and the pellets were resuspended in TRI Reagent
215 solution (Applied Biosystems, Foster City,CA, USA). After treatment with DNase I (Thermo
216 Fisher Scientific, Inc., Waltham, MA, USA), 1 µg of total RNA was reverse-transcribed using a
217 First Strand cDNA Synthesis kit (Thermo Fisher Scientific), and finally amplified using iQ™
218 SYBR® Green Supermix (Bio-Rad Laboratories, S.A., Madrid, Spain). All the procedures were
219 performed according to the manufacturers' protocols. The sequences of primer sets (forward and
220 reverse) were: glyceraldehyde-3-phosphate dehydrogenase (GAPDH), 5′-
221 GCTCTCCAGAACATCATCCC-3′ and 5′- GTCCACCACTGACACGTTG-3′; NOX4, 5′-
222 GGAAGAGCCCAGATTCCAAG-3′ and 5′-AGTCTTTCGGCACAGTACAG-3; E-Cadherin,
223 5′-ATGCTGAGGATGATTGAGGTGGGT-3′ and 5′-CAAATGTGTTCAGCTCAGCCAGCA-
224 3′. Amplification efficiencies were calculated for each pair of primers and quantification was
225 performed using the efficiency-corrected ΔΔCt method, with GAPDH as the reference gene.
226 Relative gene expression was finally expressed as folds of change compared to control cells
227 grown in the normoglycemic medium.

228 **2.11 Data presentation and statistical analysis**

229 Data were expressed as means ± standard deviation of independent experiments (n = 3). Statistical
230 analysis was performed using Statgraphics® Centurion XVI, version 16.2.04 (Statpoint
231 Technologies, Inc., Warranton, VA, USA). Shapiro-Wilk test ($p > 0.05$) was used to determine
232 the normal distribution of the dates. Student's t-test was used to determine significant differences
233 between normoglycemic and hyperglycemic for controls and WPP treatments (rWPGI, rWPF,
234 wWPGI and wWPF) and they are represented with an asterisk. One-way analysis of variance
235 (ANOVA), using Fisher's least significant difference (LSD) test, was used to determine
236 significant differences ($p < 0.05$) between data from cells incubated with the different treatments
237 in the same medium (represented with Roman for the normoglycemic medium or Greek letters
238 for the hyperglycemic medium).

239

240 **3 Results**

241 **3.1 Phenolic composition and antioxidant capacity of both red- (rWPP) and white-wine**
242 **(wWPP) digested fractions**

243 The products evaluated in this study were derived from seedless red- (rWPP) and white-wine
244 (wWPP) pomaces that were characterized in previous works [24] and are a rich source of phenolic
245 compounds (2.00 ± 0.08 and 0.95 ± 0.05 g GAE/100g respectively) (Table 1 and Table 2,
246 supporting information).

247 The total antioxidant capacity was assessed by QUENCHER methods (Q-ABTS and Q-FRAP
248 assays). Undigested pomace products (rWPP and wWPP) and their digested fractions (rWPF,
249 rWPGI, wWPGI and wWPF) *in vitro* presented the total antioxidant capacity (Table 1, supporting
250 information).

251 The phenolic compounds (phenolic acids, stilbenes, flavan-3-ols and flavonols) of the rWPP- and
252 wWPP- digested fractions are presented in Table 1 and in Table 3, supporting information. Both
253 the stilbenes and the phenolic acids were the most abundant compounds detected in the wWPP-
254 digested fractions when compared to the rWPPs, whereas flavan 3-ols were more abundant in the
255 rWPP-digested fractions. The concentration of stilbenes in the wWPGI was approximately 3-fold
256 higher than in the wWPF, while the opposite was true for the rWPP fractions where stilbene levels
257 were 1.7-fold higher in the rWPF than in the rWPGI. The total phenolic acid content was similar
258 for rWPF, wWPGI, and wWPF (275 µg/g, 289 µg/g and 311 µg/g, respectively), and the
259 hydroxybenzoic acids contributed more than the hydroxycinnamic acids to the total phenolic acid
260 content of all the WPP fractions. The dimmer levels (procyanidins B1 and B2) of the flavan-3-
261 ols subgroups were lower than the monomers (catechin, epigallocatechin and epicatechin) in both
262 fractions of rWPP, whereas the opposite was observed for the wWPP. In addition, the fermented
263 fractions of both WPPs (rWPF and wWPF) had 1.5 and 1.8-fold higher flavan-3-ols than the
264 gastrointestinal digested fractions (rWPGI and wWPGI).

265 The total flavonol content was more abundant in gastrointestinal digested fractions (9.7 and 2.3-
266 fold higher in rWPGI and wWPGI, respectively) than colonic fermentation fractions.

267 **3.2 Effects of the rWPP and wWPP-digested fractions on cell viability and proliferation.**

268 After exposure of EA.hy926 endothelial cells to 2.5 µg GAE/ml of each digested fractions
269 (rWPGI, wWPGI, rWPF and wWPF), cell viability under normo- and hyperglycemic conditions
270 was measured by MTT assay in a 24-h study (Figure 1). Cell viability remained unchanged
271 between the control and the WPPs treatments under normoglycemic conditions. However, the
272 treatment of the hyperglycemic cells with both bioavailable fractions of red and white WPPs
273 significantly prevented the cytotoxic effect observed in the hyperglycemic cells, as indicated by
274 the observable increase in the viability of the treated cells (Figure 1, full bars).

275 Furthermore, a real time study was performed, in order to evaluate the effect of the digested
276 fractions on cellular growth, using the non-invasive method xCELLigence Real-Time Cellular
277 Analysis (RTCA) system after exposure of the EA.hy926 endothelial cells to the WPP-digested
278 fractions under normoglycemic and hyperglycemic conditions (Figure 2). This system makes use
279 of impedance detection for continuous monitoring of cell viability, using the sensor electrodes
280 that are placed at the bottom of the plate for the purpose of conducting the cell adhesion and the
281 cytotoxicity studies. A higher proliferation and adhesion rate of the cells led to higher impedance
282 expressed as a cell index (CI) [27]. The WPP-digested fractions were added 24 h after seeding and
283 the viability effect was measured another 96 h. The effect of the treatment was different under
284 normo- and hyperglycemic conditions. Under normoglycemic conditions, treatment with both red
285 and white WPPs induced no cytotoxicity, as shown by the cell growing curves in the interval of
286 35 h- 75 h (Figures 2A and 2B). This observation was also confirmed by the absence of any
287 reduction in the slope curves (Figure 2C). In that regard, the addition of rWPP treatments (rWPGI
288 and rWPF) did not change the slope and the addition of the wWPP (wWPGI and wWPF) induced
289 a significant increase in the slope (Figure 2C). The hyperglycemic cells treated with the rWPP-
290 digested fractions showed no cytotoxicity throughout the 96 h of the study (Figure 2D and Figure
291 2F). However, the treatment with wWPGI showed a cytotoxicity effect of up to 40 h (Figure 2E)
292 with a significant reduction of the slope curve (64.1%) (Figure 2F).

293 **3.3 Levels of ROS and NO, and NOX4 expression in endothelial cells treated with the**
294 **digested fractions under normoglycemic and hyperglycemic conditions**

295 The gene expression of NOX4 increased more than 2-fold in EA.hy926 endothelial cells under
296 hyperglycemic conditions (Figure 3A). The treatment of hyperglycemic cells with the digested
297 fractions significantly reduced the expression of the protein NOX4. In that regard, rWPGI was
298 reduced to approximately 32.0%, rWPF to 71.7%, wWPGI to 51.9%, and wWPF to 42.0%.
299 As regards the ROS levels, the hyperglycemic cells showed a 76% increase in ROS levels (Figure
300 3B) and simultaneously, a significant 32.3% decrease in NO concentrations (Figure 3C) compared
301 to the normoglycemic cells. WPP treatments significantly reduced ROS levels by around 36-47%
302 (Figure 3B) and prevented hyperglycemia-impaired NO bioavailability (Figure 3C), as shown by
303 the higher levels of NO in the treated-cells compared to the hyperglycemic cells. The colonic
304 fermentation fractions showed the greatest differences with values that were 2.9 and 1.9 times
305 higher than the hyperglycemic cells (Figure 3C).

306 **3.4 Maintenance of endothelial adhesion evaluated by RTCA systems**

307 It is known that wine pomace-flavonoids can modulate pro-inflammatory cytokine levels,
308 improving cell survival and function. The real-time xCELLigence biosensor was used to evaluate
309 the total adhesion of the EA.hy926 endothelial cells after the treatment with INF-γ, both in the
310 presence and in the absence of the WPP-digested fractions. Total endothelial adhesion was
311 evaluated by considering two parameters: normalized cell index over time and the barrier
312 function. The normalized cell index represents the changes of impedance over time in the RTCA
313 system. The increased impedance and a normalized cell index indicated increased endothelial
314 adhesion. In addition, the barrier function indicated the percentage endothelial monolayer
315 integrity and represents the minimum cell index observed after INF-γ treatment expressed as a
316 percentage of the control cells (100%).
317 In normoglycemic EA.hy926 endothelial cells, treatment with INF-γ induced a decrease in
318 endothelial adhesion reflected by a decrease in the normalized cell index (Figure 4A I and II) and
319 a 15% reduction of the barrier function (Figure 4B I). Cell adhesion recovery took place 15 h after

320 treatment with INF-γ. The cells were pre-treated for 4 h with the rWPP and wWPP-digested
321 fractions, 4 h before treatment with INF-γ, for the evaluation of the WPPs and their protective
322 effects. The results (Figure 4A I) showed that treatment with both the rWPGI and the rWPF
323 fractions induced an increase in endothelial adhesion over approximately 8 h and 5 h for the
324 rWPGI and the rWPF, respectively, after activation with INF-γ (Figure 4A I). Furthermore, the
325 reduction in the barrier function was significantly lower for rWPGI (13%) compared with INF-γ
326 alone (Figure 4B I). Treatment with the wWPP-digested fractions (wWPF and wWPGI) after
327 treatment with INF-γ resulted in decreased cell adhesion (15% and 12%, respectively) (Figure 4A
328 II and 4A I) with recovery of endothelial adhesion after 14 h and after 8 h, for wWPGI and for
329 wWPF, respectively (Figure 4A II). These results showed that the treatments with WPPs
330 prevented the INF-γ effect on barrier integrity, thereby reducing the decrease in impedance and
331 the time to recovery, thereby improving cell adhesion. A comparison of the different WPPs
332 fractions showed that the major preventive effect against INF-γ was more marked for the wWPF.
333 In the hyperglycemic endothelial cells, INF-γ caused a marked increase in permeability, as
334 observed in Figures 4A II and 4A II, decreasing endothelial adhesion and reducing the barrier
335 function by 24% (Figures 4A II and 4B II). The pre-treatment of hyperglycemic EA.hy926 cells
336 with rWPP-digested fractions prevented any decrease of cell adhesion induced by INF-γ (Figure
337 4B II), obtaining a 20% reduction and reaching the control adhesion levels at 14 h for rWPGI and
338 8 h for rWPF (Figure 4A III). A similar barrier function protective effect was observed for the
339 pre-treatment with wWPF, with an increase of cell adhesion until 17 h after INF-γ treatment
340 (Figure 4A IV). However, pre-treatment with wWPGI resulted in the lowest decrease of adhesion
341 after INF-γ treatment (6%) with an increase during 7 h (Figure 4A IV and 4B II). Those results
342 indicated that the major barrier vascular protective effect against the INF-γ effect under
343 hyperglycemic conditions was shown by wWPGI.

344 **3.5 Levels of ROS and NO, and NOX4 expression in endothelial cells treated with the**
345 **digested fractions and interferon gamma under normo- and hyperglycemic conditions**

346 The gene expression of NOX4 was significantly increased by interferon in both EA.hy926
347 endothelial cells under normoglycemic and hyperglycemic conditions (3.5 and 2.0 times higher
348 compared with the controls, respectively) (Figure 5A). The treatment of normoglycemic cells
349 with the digested fractions before interferon addition, reduce the gene expression of NOX4
350 reaching the normoglycemic control level. All digested fractions significantly reduced the
351 expression of the protein NOX4 in the hyperglycemic cells treated with the interferon. In that
352 regard, red fractions exhibited the more marked reduction (76% for the rWPGI and 79% for the
353 rWPF) while both wWPP fractions showed a 68% of reduction of NOX4 expression.
354 In another hand, the ROS levels agreed with the NOX4 expression levels, showing an increase in
355 cells exposed to interferon in both normoglycemic and hyperglycemic cells (Figure 5B). Under
356 normoglycemic conditions, all digested fractions reduce the ROS levels in presence of interferon,
357 and these were more marked for the rWPGI and wWPF fractions (30% and 35%, respectively).
358 WPP treatments have a similar action in hyperglycemic cells treated with interferon, and
359 significantly reduced ROS levels by around 47%. Remarkably, the rWPF fraction showed the
360 highest reduction of both NOX4 and ROS levels under hyperglycemic conditions (79% and 47%,
361 respectively).
362 Interestingly, total nitric oxide (NO) production (Figure 5C) by normoglycemic cells was
363 increased by interferon in about 28%, and two of the digested fractions (rWPF and wWPGI)
364 exhibited a significatively reduction and reached the control levels. However, under
365 hyperglycemic conditions these increase in the NO level by interferon was lower and three of the
366 digested fractions (rWPF, wWPGI and wWPF) produce a significatively reduction (about 30%
367 less than interferon) reaching control levels.
368 **3.6 Effects of red and white WPPs on adherent junctions**
369 The vascular barrier protective effect observed in the endothelial cells was tested, by the
370 evaluation of the actin cytoskeleton and cell-cell adherent protein E-cadherin at 1.5 hours after
371 treatment with INF-γ and the pre-treatment effects of both the rWPP and the wWPP-digested
372 fractions.

373 The normal cobblestone morphology of the EA.hy926 cells was observed both under
374 normoglycemic (Figure 6A I) and under hyperglycemic (Figure 6A III) conditions. The actin
375 cytoskeleton and E-cadherin cell-cell junctions of the endothelial monolayer were studied by
376 immunofluorescence. Gene expression of E-cadherin was also studied by real-time PCR.
377 Under normoglycemic conditions, the cell morphology, the distribution of actin, and the E-
378 cadherin levels (protein and mRNA) all significantly changed following treatment with INF-γ. In
379 comparison with normoglycemic control, both the actin cortex and the cobblestone morphology
380 were less marked (Figure 6A II and 6B II); the number of intercellular spaces increased by around
381 145% (Figure 6C I); stress fibers were evident (Figure 6B II, white arrows); and, a decrease (78%)
382 in the E-cadherin cell-cell junctions (Figure 6B II, Figure 6D I) and E-cadherin gene expression
383 (Figure 6E I) were observed. Pre-treatment of the normoglycemic cells with the rWPP and the
384 wWPP-digested fractions (rWPGI, rWPF, wWPGI, and wWPF) showed lower intercellular
385 spaces (Figure 6C I) than the control cells and similar actin distribution patterns (Figure 6B III-
386 VI), indicating a protective effect against the INF-γ–induced changes. As regards the effect on
387 the E-cadherin cell-cell junctions, pre-treatment with the rWPF, wWPGI and wWPF reverted the
388 damage of the INF-γ by increasing the E-cadherin junctions (Figure 6B IV-VI and Figure 6D I)
389 and E-cadherin expression (Figure 6E I). In contrast, the rWPGI showed no protective effect on
390 the cell-cell junction with similar E-cadherin levels between the INF-γ and the INF-γ+rWPGI
391 treated cells (Figure 6B III, 6D I and 6E I). These results agree with those observed in the
392 impedance curve, in which the impedance levels of the rWPGI pre-treated cells decreased to
393 similar levels as the INF-γ at 1.5 hours post-stimulation.
394 The morphology of EA.hy926 hyperglycemic endothelial cells and the staining of both actin and
395 E-cadherin are shown in Figure 6A III and Figure 6B VII, respectively. Exposure of the
396 hyperglycemic cells to INF-γ showed a change in their morphology, as may be seen in Figure 6B
397 VIII, with an altered actin distribution, incremented cell-cell spaces of about 392% (Figure 6C
398 II), and a decrease in the E-cadherin cell-cell junction (Figure 6B VIII) with a 63% decrease of
399 E-cadherin fluorescence levels (Figure 6D II) and about 54% of E-cadherin gene expression

400 (Figure 6E II). Hyperglycemic cell pre-treatment with the WPP-digested fractions resulted in a
401 protective effect against cell damage provoked by INF-γ. The cells revealed a monolayer similar
402 to the hyperglycemic control cells with a cobblestone morphology, decreased morphological
403 rearrangement of the actin filaments compared with the INF-γ-non-treated cells (Figure 6B IX-
404 XII), fewer intercellular spaces (Figure 6C II), and similar distributions and levels of E-cadherin
405 to the control samples (Figure 6B IX-XII, Figure 6D II and Figure 6E II). Those results also
406 agreed with the results observed after the impedance assays. Interestingly, the wWPGI fraction
407 that had the highest protective effect against impedance, also showed the highest levels of E-
408 cadherin cell-cell junctions (Figure 6D II and Figure 6E II).
409 In summary, the treatment of both normoglycemic and hyperglycemic cells with the WPP-
410 digested fractions preserved the actin cytoskeleton, the E-cadherin junctions, and their cellular
411 morphology against the effects of the INF-γ.
412
413
414
415 **4 Discussion**
416 The endothelium forms a selective barrier between the bloodstream and the surrounding tissues.
417 Changes to that biological barrier alter endothelium functionality leading to endothelial
418 dysfunction and contributing to the pathogenesis of several disorders such as cardiovascular
419 diseases [28,29]. This could be a consequence of changes to oxidative stress levels that can alter the
420 balance of nitric oxide and damage the endothelium, thereby increasing its permeability [29,30].
421 Phenolic compounds of WPP-digested fractions, WPGI and WPF, revealed that the fraction
422 obtained from colonic fermentation, WPF, for both, rWPP and wWPP, had a high content of non-
423 flavonoid hydroxycinnamic acids and flavan 3-ols, unlike the gastrointestinal digestion products
424 (WPGI) that had a higher content of flavonols. The higher content of phenolic acids in the colonic
425 fermentation fractions may be a consequence of intestinal microorganisms actions that release
426 and modify these compounds [31]. Moreover, both red wine pomace fractions (rWPGI and rWPF)

427 are more abundant in monomeric flavan-3-ols (catechin, epigallocatechin and epicatechin), while
428 the wWPGI is rich in hydroxycinnamic acids and stilbenes (resveratrol). Therefore, the phenolic
429 profile is dependent on the type of WPP and its bioaccessibility. It is important to point out that
430 the wine pomaces suffered an *in vitro* digestion and the bioavailability can be different for *in vivo*
431 models. As we demonstrated in previous *in vivo* studies in Wistar rats [24,32], the bioavailability of
432 the rWPP not increase with the dose and it was similar than the observed in the *in vitro* digestion
433 performed in the present study (around 2 µg gallic acid/g rWPP). However, the bioavailability of
434 the wWPP depends of the dose and differ between the *in vivo* (14.8 µg gallic acid/g wWPP) and
435 the *in vitro* (2.02 µg gallic acid/g wWPP) digestion process. For this, the results obtained from
436 the *in vitro* digested products must considered as an approximation to the potentially observed *in*
437 *vivo*.
438 The hyperglycemic effect on EA.hy926 endothelial cells is well established and it is characterized
439 by decreased cell proliferation and increased apoptosis, due to higher oxidative stress levels [33].
440 Our results showed that this effect was regulated by all fractions of WPPs, in which the WPP
441 fractions increased the cell viability of the hyperglycemic cells (24 hours study) and regulated
442 cell proliferation in a real-time study of 120 hours. The correct functioning of the vascular
443 endothelium depends on the balance between nitric oxide (NO) and the free radical levels of the
444 endothelial cells [34]. In this work, we found that the treatment of EA.hy926 endothelial cells with
445 the WPPs fractions in non-stressed conditions promoted NO generation, thus stimulating the
446 vasodilatation that could increase the cAMP levels and promote enhanced endothelial barrier
447 functions, probably by inhibition of RhoA [3] and ROS generation [35]. Phenolic compounds present
448 in the wine pomace products showed preventive and/or restorative effect of the on endothelial
449 barrier damage to regulate endothelial permeability, by preserving NO, either by direct
450 scavenging of ROS, and/or by helping to prevent NOX4-generated superoxide and subsequent
451 peroxinitritite formation. The tendency of wine pomace products to reduce ROS levels and
452 downregulate NOX4 expression is in agreement with previous studies of endothelial cells exposed
453 to hyperglycemia [8,15] and *in vivo* models of oxidative stress-related diseases [36,37] and could be a

454 consequence of the modulation of several cellular pathways such as NF-κB and Nrf2 by phenolic
455 compounds of the wine pomace products such as hydroxycinnamic acids, resveratrol, epicatechin,
456 and procyanidins [38–42].
457 Moreover, endothelium acts as a selective barrier between plasma and the interstitial space, which
458 can be altered by increased ROS levels and imbalanced NO levels as consequence of
459 inflammatory processes. Therefore, one of most evident effects of endothelial dysfunction is its
460 increased permeability, due to changes in the adhesion cells, allowing the extravasations of larger
461 molecules through the endothelial cells [43]. Inflammatory mediators such as INF-γ or
462 hyperglycemia modulate the expression of several cellular pathways involved in the regulation of
463 NO/ROS balance through the modulation of enzymes such as NOX4, eNOS and iNOS [44–48]. This
464 effect could be modulating by rWPF and the wWPGI phenolic compounds whose structural
465 characteristics determine the capacity to scavenging and inhibiting ROS and NOX4 [42]. Hence, the
466 polyphenols catechin, epicatechin and quercetin (withouth substitutions in the B ring) are good
467 scavengers of superoxide radicals [42]. On the other hand, resveratrol and hydroxycinnamic acids
468 such as caffeic and ferulic acids (with substitutions in the B ring and presence of a hydroxyl or
469 methyl group in an aromatic ring) could be responsible for NOX4 inhibition prompted by rWPF
470 and wWPGI observed. Remarkably, rWPF fraction, with a high content of ferulic acid, highlights
471 the highest reduction of both NOX4 and ROS levels in cells exposed to both pro-inflammatory
472 mediators (hyperglycemia and INF-γ). Moreover, these results agree with other studies[8,42,49,50] and
473 suggest that the inhibition of NOX4/ROS by polyphenols is modulated by NF-κB pathway.
474 Despite NOX4/ROS generation, the other crucial component of the endothelial dysfunction is the
475 nitric oxide (NO), which reduction is implicated in the increase of vascular permeability [48,51]. It
476 was expected a reduction of the NO levels by the pro-inflammatory mediators, however, the
477 different behavior of hyperglycemia and interferon, in which while hyperglycemia reduce NO
478 levels, interferon increase them, could be attributed to different cellular pathways modulated by
479 these two mediators. It was demonstrated in previous studies that hyperglycemia and interferon
480 could reduce NO levels by downregulation of endothelial nitric oxide synthase (eNOS)

481 expression[46,47,52]. However, interferon could also increase the levels of NO, in the normoglycemic
482 EA.hy926 cells, by upregulation of the expression of the pro-inflammatory inducible nitric oxide
483 synthase (iNOS) enzyme [44,53,54]. Several polyphenols of the WPP showed an inhibitory effect on
484 iNOS [55–57] through downregulation of NF-κB/Akt/iNOS pathway. Interestingly, in agree with
485 other studies [57–59] that demonstrated an inhibitory effect of caffeic acid on iNOS, the fraction with
486 the more marked effect against interferon increased-NO levels (rWPGI in normoglycemic
487 conditions) was that with the highest content of this phenolic acid.
488 Furthermore, it is known that increased permeability caused by IFN-γ is due to RhoA-ROCK-
489 dependent actin reorganization and to an increase in the endocytosis of tight junction components
490 such as E-cadherin [60,61]. The WPP fractions counter the loss of cell adhesion and barrier integrity
491 induced by INF-γ in normo- and hyperglycemic conditions, mainly highlighting the protective
492 effect observed for the wWPP-digested fractions. The high content of resveratrol, procyanidins,
493 hydroxycinnamic acids and flavonols such as quercetin in wWPGI and wWPF could be involved
494 in this endothelial protection process, by inhibition of pro-inflammatory cytokines [62] or inhibition
495 of the JAK/STAT, PI3K and MAPK pathways [63]; both of which are mechanisms involved in the
496 disturbance of vascular permeability due to INF-γ.
497 In addition, immunofluorescence experiments corroborated those observations, indicating that the
498 protective effect of wine pomace products on cell permeability was due, at least in part, to its
499 ability to sustain the adherens junctions and counteract the alterations in the actin cytoskeleton
500 under hyperglycemic and pro-inflammatory conditions. It is known that junction proteins
501 (adherens and tight junctions) together with polymerized cytoskeletons are critical for the
502 maintenance of the endothelial barrier [64] and any disruption or disorganization weakens the
503 endothelial barrier and leads to endothelial dysfunction [64]. Both the structure and the function of
504 adherens junctions are sensitive to a number of stimuli, including oxidative stress damage [30] and
505 inflammatory cytokines such as INF-γ, which can contribute to increased vessel permeability
506 through down-regulation of E-cadherin, leading to the extravasation of macromolecules [65,66].
507 Those results agree with our results where INF-γ increased EA.hy926 endothelial cell monolayer

508 permeability and modified the cell morphology correlated with down-regulation of E-cadherin,
509 as well as introducing major changes to the actin cytoskeleton, as revealed by phalloidin staining.
510 WPPs attenuated the permeability of the endothelial cells induced by INF-γ and were partially
511 able to reduce the disorganization of E-Cadherin and actin-cytoskeleton. It is known, that the
512 WPPs polyphenols resveratrol (stilbene), epigallocatechin gallate (flavan-3-ol), and caffeic acid
513 (hydroxycinnamic acid) increase E-cadherin expression and improve cell-cell junctions,
514 preserving the endothelial cell barrier [67,68]. Considering that it has been proposed an association
515 between the activation of the Nrf2 pathway and the upregulation of E-cadherin expression [69], the
516 upregulation of Nrf2 by wine pomace products[8] could to explain the preservation of the
517 endothelial barrier by these products through the increased expression of E-cadherin by the WPP.
518 Furthermore, the highest content of phenolic acids of the wWPP-digested fractions and the highest
519 content of resveratrol of the wWPGI and rWPF could explain the effects observed in the E-
520 cadherin distribution and gene expression, and actin cytoskeleton morphology after treatment
521 with these fractions.
522 In summary, we have demonstrated the protective effects of WPPs against hyperglycemic and
523 inflammatory cytokine-induced cellular damage in endothelial cells. These positive outcomes
524 were very likely the result of the combined effects of (1) decreased ROS production, thus
525 maintaining the cellular redox balance and cellular oxidation levels; (2) stabilization of junction
526 proteins via their modulation; and, (3) the maintenance of the cytoskeleton structure.

527 **5 Concluding remarks**

528 Our findings in this paper have pointed to the inhibitory effects of both rWPP and wWPP on high
529 glucose-mediated endothelial damage. The prevention of INFγ-induced barrier disruption by each
530 compound has therefore added further weight to the potentially protective effects of those
531 products against vascular inflammatory diseases.

532

533 **6 Abbreviations**

534 NO, nitric oxide; ROS, reactive oxygen species; NOX4, NADPH oxidase 4; rWPP, red wine
535 pomace product; EA.hy926 endothelial cells, human umbilical vein endothelial cells; VE-
536 cadherin, vascular endothelial cadherin; INF-γ, gamma interferon; rWPP, red wine pomace
537 product; wWPP, white wine pomace product; rWPGI, potentially bioavailable gastrointestinal
538 digestion fraction of the red wine pomace product; rWPF, potentially bioavailable colonic
539 fermentation fraction of the red wine pomace product; wWPGI, potentially bioavailable
540 gastrointestinal digestion fraction of the white wine pomace product; wWPF, potentially
541 bioavailable colonic fermentation fraction of the red wine pomace product.
542

543 **7 Acknowledgments**

544 The authors thank the financial support of the Spain Ministry of Science, Innovation and
545 Universities (Ref. PGC2018-097113-B-I00).
546

547 **8 Appendix: Supporting Information**

548 Supporting Information data to this article: Table 1, Supporting Information. Composition and
549 total antioxidant capacity (TAC) of seedless red wine pomace product (rWPP) and white wine
550 pomace product (wWPP) and their gastrointestinal (WPGI) and colonic fermentation (WPF)
551 digested fractions. Table 2, Supporting Information. Phenolic composition of the red (rWPP) and
552 white (wWPP) wine pomace products assayed by GC/MS/MS and HPLC/DAD. Table 3,
553 Supporting Information. Phenolic composition of the red (rWPP) and white (wWPP) wine
554 pomace products digested fraction assayed by GC/MS/MS.
555

556 **9 Conflicts of interest**

557 The authors declare no conflict of interest.
558

559 **10 References**

560 1 H. Patel, J. Chen, K. C. Das and M. Kavdia, Hyperglycemia induces differential change

in oxidative stress at gene expression and functional levels in HUVEC and HMVEC, *Cardiovascular Diabetology*, 2013, **12**, 1. https://doi.org/10.1186/1475-2840-12-142.

2 M. Simionescu, Implications of Early Structural-Functional Changes in the Endothelium for Vascular Disease, *Arteriosclerosis, Thrombosis, and Vascular Biology*, 2007, **27**, 266–274. https://doi.org/10.1161/01.ATV.0000253884.13901.e4.

3 M. Giannotta, M. Trani and E. Dejana, Review VE-Cadherin and Endothelial Adherens Junctions : Active Guardians of Vascular Integrity, *Developmental Cell*, 2013, **26**, 441–454. https://doi.org/10.1016/j.devcel.2013.08.020.

4 G. Bazzoni and E. Dejana, Endothelial Cell-to-Cell Junctions : Molecular Organization and Role in Vascular Homeostasis, *Phytochemistry Reviews*, 2004, **84**, 869–901.

5 F. Chen, L. H. Qian, B. Deng, Z. M. Liu, Y. Zhao and Y. Y. Le, Resveratrol protects vascular endothelial cells from high glucose-induced apoptosis through inhibition of nadph oxidase activation-driven oxidative stress, *CNS Neuroscience and Therapeutics*, 2013, **19**, 675–681. https://doi.org/10.1111/cns.12131.

6 P. K. Bagul, N. Deepthi, R. Sultana and S. K. Banerjee, Resveratrol ameliorates cardiac oxidative stress in diabetes through deacetylation of NFkB-p65 and histone 3, *Journal of Nutritional Biochemistry*, 2015, **26**, 1298–1307. https://doi.org/10.1016/j.jnutbio.2015.06.006.

7 N. Suganya, E. Bhakkiyalakshmi, D. V. L. Sarada and K. M. Ramkumar, Reversibility of endothelial dysfunction in diabetes : role of polyphenols, *British Journal of Nutrition*, 2016, **116**, 223–246. https://doi.org/10.1017/S0007114516001884.

8 G. Gerardi, M. Cavia-Saiz, M. D. Rivero-Pérez, M. L. González-SanJosé and P. Muñiz, Modulation of Akt-p38-MAPK/Nrf2/SIRT1 and NF-κB pathways by wine pomace product in hyperglycemic endothelial cell line, *Journal of Functional Foods*, 2019, **58**, 255–265. https://doi.org/10.1016/j.jff.2019.05.003.

9 R. Y. Kiseleva, P. M. Glassman, C. F. Greineder, E. D. Hood, V. V. Shuvaev and V. R. Muzykantov, Targeting therapeutics to endothelium: are we there yet?,*Targeting*

588 *therapeutics to endothelium: are we there yet?*, 2018, vol. 8.
589 https://doi.org/10.1007/s13346-017-0464-6.
590 10 A. Daiber, S. Steven, A. Weber, V. V. Shuvaev, V. R. Muzykantov, I. Laher, H. Li, S.
591 Lamas and T. Münzel, Targeting vascular (endothelial) dysfunction, *British Journal of*
592 *Pharmacology*, 2017, **174**, 1591–1619. https://doi.org/10.1111/bph.13517.
593 11 M. A. Kaisar, S. Prasad and L. Cucullo, Protecting the BBB Endothelium against
594 Cigarette Smoke- Induced Oxidative Stress Using Popular Antioxidants: Are they really
595 beneficial?, *Brain Research*, 2015, **1627**, 90–100.
596 https://doi.org/10.1016/j.physbeh.2017.03.040.
597 12 S. Steven, K. Frenis, M. Oelze, S. Kalinovic, M. Kuntic, M. T. Bayo Jimenez, K.
598 Vujacic-Mirski, J. Helmstädter, S. Kröller-Schön, T. Münzel and A. Daiber, Vascular
599 Inflammation and Oxidative Stress: Major Triggers for Cardiovascular Disease,
600 *Oxidative Medicine and Cellular Longevity*, 2019, **2019**, 1–26.
601 https://doi.org/10.1155/2019/7092151.
602 13 J. Egea, I. Fabregat, Y. M. Frapart, P. Ghezzi, A. Görlach, T. Kietzmann, K. Kubaichuk,
603 et al., European contribution to the study of ROS: A summary of the findings and
604 prospects for the future from the COST action BM1203 (EU-ROS), *Redox Biology*,
605 2017, **13**, 94–162. https://doi.org/10.1016/j.redox.2017.05.007.
606 14 M. Wojtala, L. Pirola and A. Balcerczyk, Modulation of the vascular endothelium
607 functioning by dietary components , the role of epigenetics, *BioFactors*, 2016, 1–12.
608 https://doi.org/10.1002/biof.1306.
609 15 R. Del Pino-García, G. Gerardi, M. D. Rivero-Pérez, M. L. González-SanJosé, J. García-
610 Lomillo and P. Muñiz, Wine pomace seasoning attenuates hyperglycaemia-induced
611 endothelial dysfunction and oxidative damage in endothelial cells, *Journal of Functional*
612 *Foods*, 2016, **22**, 431–445. https://doi.org/10.1016/j.jff.2016.02.001.
613 16 I. Rahman, S. K. Biswas and P. A. Kirkham, Regulation of inflammation and redox
614 signaling by dietary polyphenols, *Biochemical Pharmacology*, 2006, **72**, 1439–1452.

https://doi.org/10.1016/j.bcp.2006.07.004.

17 R. Del Pino-García, J. García-Lomillo, M. D. Rivero-Pérez, M. L. González-Sanjosé and P. Muñiz, Adaptation and Validation of QUick, Easy, New, CHEap, and Reproducible (QUENCHER) Antioxidant Capacity Assays in Model Products Obtained from Residual Wine Pomace, *Journal of Agricultural and Food Chemistry*, 2015, **63**, 6922–6931. https://doi.org/10.1021/acs.jafc.5b01644.

18 H. M. Hügel, N. Jackson, B. May, A. L. Zhang and C. C. Xue, Polyphenol protection and treatment of hypertension, *Phytomedicine*, 2016, **23**, 220–231. https://doi.org/10.1016/j.phymed.2015.12.012.

19 Sazonador de origen vegetal con propiedades conservantes, sustitutivo de la sal, y procedimiento de obtención del mismo,2013, Spain Patent ES2524870 B.

20 J. García-Lomillo, M. L. González-SanJosé, R. Del Pino-García, M. D. Rivero-Pérez and P. Muñiz-Rodríguez, Antioxidant and antimicrobial properties of wine byproducts and their potential uses in the food industry, *Journal of Agricultural and Food Chemistry*, 2014, **62**, 12595–12602. https://doi.org/10.1021/jf5042678.

21 S. Pérez-Magariño, M. Ortega-Heras and E. Cano-Mozo, Optimization of a solid-phase extraction method using copolymer sorbents for isolation of phenolic compounds in red wines and quantification by HPLC, *Journal of Agricultural and Food Chemistry*, 2008, **56**, 11560–11570. https://doi.org/10.1021/jf802100j.

22 R. Abu-Amsha Caccetta, V. Burke, T. A. Mori, L. J. Beilin, I. B. Puddey and K. D. Croft, Red wine polyphenols, in the absence of alcohol, reduce lipid peroxidative stress in smoking subjects, *Free Radical Biology and Medicine*, 2001, **30**, 636–642. https://doi.org/10.1016/S0891-5849(00)00497-4.

23 A. Scalbert and G. Williamson, Dietary Intake and Bioavailability of Polyphenols, *The Journal of Nutrition*, 2000, **130**, 2073–2085. https://doi.org/10.1089/109662000416311.

24 G. Gerardi, M. Cavia-Saiz, M. D. Rivero-Pérez, M. L. González-SanJosé and P. Muñiz, The dose–response effect on polyphenol bioavailability after intake of white and red

642 wine pomace products by Wistar rats, *Food & Function*, 2020, 1661–1671.
643 https://doi.org/10.1039/c9fo01743g.
644 25 P. R. Twentyman and M. Luscombe, A study of some variables in a tetrazolium dye
645 (MTT) based assay for cell growth and chemosensitivity, *British Journal of Cancer*,
646 1987, **56**, 279–285. https://doi.org/10.1038/bjc.1987.190.
647 26 H. Wang and J. A. Joseph, Quantifying cellular oxidative stress by dichlorofluorescein
648 assay using microplate reader, *Free Radical Biology and Medicine*, 1999, **27**, 612–616.
649 27 M. Roshan Moniri, A. Young, K. Reinheimer, J. Rayat, L. J. Dai and G. L. Warnock,
650 Dynamic assessment of cell viability, proliferation and migration using real time cell
651 analyzer system (RTCA), *Cytotechnology*, 2015, **67**, 379–386.
652 https://doi.org/10.1007/s10616-014-9692-5.
653 28 C. Premer, A. J. Kanelidis, J. M. Hare and I. H. Schulman, Rethinking Endothelial
654 Dysfunction as a Crucial Target in Fighting Heart Failure, *Mayo Clinic Proceedings:*
655 *Innovations, Quality & Outcomes*, 2019, **3**, 1–13.
656 https://doi.org/10.1016/j.mayocpiqo.2018.12.006.
657 29 Y. A. Komarova, K. Kruse, D. Mehta, A. B. Malik and V. Biology, Protein interactions
658 at endothelial junctions and signaling mechanisms regulating endothelial permeability,
659 *Circulation Research*, 2018, **120**, 179–206.
660 https://doi.org/10.1161/CIRCRESAHA.116.306534.Protein.
661 30 H. Gong, X. Gao, S. Feng, M. R. Siddiqui, A. Garcia, M. G. Bonini, Y. Komarova, S. M.
662 Vogel, D. Mehta and A. B. Malik, Evidence of a common mechanism of disassembly of
663 adherens junctions through Ga13 targeting of VE-cadherin, *The Journal of Experimental*
664 *Medicine*, 2014, **211**, 579–591. https://doi.org/10.1084/jem.20131190.
665 31 F. Saura-Calixto, J. Serrano and I. Goñi, Intake and bioaccessibility of total polyphenols
666 in a whole diet, *Food Chemistry*, 2007, **101**, 492–501.
667 https://doi.org/10.1016/j.foodchem.2006.02.006.
668 32 R. Del Pino-García, M. D. Rivero-Pérez, M. L. González-SanJosé, K. D. Croft and P.

669 Muñiz, Bioavailability of phenolic compounds and antioxidant effects of wine pomace
670 seasoning after oral administration in rats, *Journal of Functional Foods*, 2016, **25**, 486–
671 496. https://doi.org/10.1016/j.jff.2016.06.030.
672 33 K. K. J. Senthil, V. M. Gokila and S. Wang, Activation of Nrf2-mediated anti-oxidant
673 genes by antrodin C prevents hyperglycemia-induced senescence and apoptosis in
674 human endothelial cells,2017, **8**, 96568–96587.
675 34 S. Jamwal and S. Sharma, Vascular endothelium dysfunction: a conservative target in
676 metabolic disorders, *Inflammation Research*, 2018, **67**, 391–405.
677 https://doi.org/10.1007/s00011-018-1129-8.
678 35 B. M. Fu, J. Yang, B. Cai, J. Fan, L. Zhang and M. Zeng, Reinforcing endothelial
679 junctions prevents microvessel permeability increase and tumor cell adhesion in
680 microvessels in vivo, *Scientific Reports*, 2015, **5**, 1–12.
681 https://doi.org/10.1038/srep15697.
682 36 R. Del Pino-García, M. D. Rivero-Pérez, M. L. González-SanJosé, K. D. Croft and P.
683 Muñiz, Antihypertensive and antioxidant effects of supplementation with red wine
684 pomace in spontaneously hypertensive rats, *Food & Function*, 2017, **8**, 2444–2454.
685 https://doi.org/10.1039/C7FO00390K.
686 37 R. Del Pino-García, M. D. Rivero-Pérez, M. L. González-Sanjosé, P. Castilla-Camina,
687 K. D. Croft and P. Muñiz, Attenuation of oxidative stress in Type 1 diabetic rats
688 supplemented with a seasoning obtained from winemaking by-products and its effect on
689 endothelial function, *Food and Function*, 2016, **7**, 4410–4421.
690 https://doi.org/10.1039/c6fo01071g.
691 38 C. G. Fraga, P. I. Oteiza and M. Galleano, Plant bioactives and redox signaling: (–)-
692 Epicatechin as a paradigm, *Molecular Aspects of Medicine*, 2018, **61**, 31–40.
693 https://doi.org/10.1016/j.mam.2018.01.007.
694 39 S. Mateen, S. Moin, A. Zafar and A. Q. Khan, Redox signaling in rheumatoid arthritis
695 and the preventive role of polyphenols, *Clinica Chimica Acta*, 2016, **463**, 4–10.

696 https://doi.org/10.1016/j.cca.2016.10.007.
697 40 S. V. Verstraeten, G. G. Mackenzie, P. I. Oteiza and C. G. Fraga, (-)-Epicatechin and
698 related procyanidins modulate intracellular calcium and prevent oxidation in Jurkat T
699 cells, *Free Radical Research*, 2008, **42**, 864–872.
700 https://doi.org/10.1080/10715760802471452.
701 41 D. Tagliazucchi, E. Verzelloni and A. Conte, The first tract of alimentary canal as an
702 extractor. release of phytochemicals from solid food matrices during simulated digestion,
703 *Journal of Food Biochemistry*, 2012, **36**, 555–568. https://doi.org/10.1111/j.1745-
704 4514.2011.00569.x.
705 42 A. Serino and G. Salazar, Protective Role of Polyphenols against Vascular Inflammation
706 , Aging and Cardiovascular Disease, *Nutrients*, 2019, **11**, 1–23.
707 https://doi.org/10.3390/nu11010053.
708 43 L. Claesson-welsh and L. Claesson-welsh, Vascular permeability — the essentials
709 Vascular permeability — the essentials, *Upsala Journal of Medical Sciences*, 2015, **120**,
710 135–143. https://doi.org/10.3109/03009734.2015.1064501.
711 44 E. M. Coccia, E. Stellacci, G. Marziali, G. Weiss and A. Battistini, IFN-γ and IL-4
712 differently regulate inducible NO synthase gene expression through IRF-1 modulation,
713 *International Immunology*, 2000, **12**, 977–985. https://doi.org/10.1093/intimm/12.7.977.
714 45 Y. Takada, A. Mukhopadhyay, G. C. Kundu, G. H. Mahabeleshwar, S. Singh and B. B.
715 Aggarwal, Hydrogen peroxide activates NF-κB through tyrosine phosphorylation of
716 IκBα and serine phosphorylation of p65., *Journal of Biological Chemistry*, 2003, **278**,
717 24233–24241. https://doi.org/10.1074/jbc.M212389200.
718 46 X. L. Du, D. Edelstein, S. Dimmeler, Q. Ju, C. Sui and M. Brownlee, Hyperglycemia
719 inhibits endothelial nitric oxide synthase activity by posttranslational modification at the
720 Akt site, *Journal of Clinical Investigation*, 2001, **108**, 1341–1348.
721 https://doi.org/10.1172/JCI11235.
722 47 J. J. Buie, L. L. Renaud, R. Muise-Helmericks and J. C. Oates, Interferon-α Negatively

723 Regulates the Expression of Endothelial Nitric Oxide Synthase and Nitric Oxide
724 Production: Implications for SLE, *Physiology & Behavior*, 2018, **176**, 139–148.
725 https://doi.org/10.1016/j.physbeh.2017.03.040.
726 48 C. T. Ng, L. Y. Fong, Y. Y. Low, J. Ban, M. N. Hakim and Z. Ahmad, Nitric oxide
727 participates in ifn-γ -induced huvecs hyperpermeability, *Physiological Research*, 2016,
728 **65**, 1053–1058. https://doi.org/10.33549/physiolres.933237.
729 49 M. A. Alam, N. Subhan, H. Hossain, M. Hossain, H. M. Reza, M. M. Rahman and M. O.
730 Ullah, Hydroxycinnamic acid derivatives: A potential class of natural compounds for
731 the management of lipid metabolism and obesity, *Nutrition and Metabolism*, 2016, **13**,
732 1–13. https://doi.org/10.1186/s12986-016-0080-3.
733 50 C. Li, L. Li, C. fang Yang, Y. juan Zhong, D. Wu, L. Shi, L. Chen and Y. wen Li,
734 Hepatoprotective effects of Methyl ferulic acid on alcohol-induced liver oxidative injury
735 in mice by inhibiting the NOX4/ROS-MAPK pathway, *Biochemical and Biophysical*
736 *Research Communications*, 2017, **493**, 277–285.
737 https://doi.org/10.1016/j.bbrc.2017.09.030.
738 51 J. Tejero, S. Shiva and M. T. Gladwin, Sourcesof vascular nitric oxide and reactive
739 oxygen species and their regulation, *Physiological Reviews*, 2019, **99**, 311–379.
740 52 F. Lin, Y. Yang, S. Wei, X. Huang, Z. Peng, X. Ke, Z. Zeng and Y. Song, Hydrogen
741 sulfide protects against high glucose-induced human umbilical vein endothelial cell
742 injury through activating PI3K/Akt/eNOS pathway, *Drug Design, Development and*
743 *Therapy*, 2020, **14**, 621–633. https://doi.org/10.2147/DDDT.S242521.
744 53 M. M. Remy, M. Sahin, L. Flatz, T. Regen, L. Xu, M. Kreutzfeldt, B. Fallet, C. Doras,
745 T. Rieger, L. Bestmann, U. K. Hanisch, B. A. Kaufmann, D. Merkler and D. D.
746 Pinschewer, Interferon-γ-Driven iNOS: A Molecular Pathway to Terminal Shock in
747 Arenavirus Hemorrhagic Fever, *Cell Host and Microbe*, 2017, **22**, 354-365.e5.
748 https://doi.org/10.1016/j.chom.2017.07.008.
749 54 T. Salim, C. L. Sershen and E. E. May, Investigating the role of TNF-α and IFN-γ

750 activation on the dynamics of iNOS gene expression in lps stimulated macrophages,
751 *PLoS ONE*, , DOI:10.1371/journal.pone.0153289.
752 https://doi.org/10.1371/journal.pone.0153289.
753 55 T. De Bruyne, B. Steenput, L. Roth, G. R. Y. De Meyer, C. N. Dos Santos, K.
754 Valentová, M. Dambrova and N. Hermans, Dietary polyphenols targeting arterial
755 stiffness: Interplay of contributing mechanisms and gut microbiome-related Metabolism,
756 *Nutrients*, 2019, **11**, 1–43. https://doi.org/10.3390/nu11030578.
757 56 J. Paixão, T. C. P. Dinis and L. M. Almeida, Malvidin-3-glucoside protects endothelial
758 cells up-regulating endothelial NO synthase and inhibiting peroxynitrite-induced NF-kB
759 activation, *Chemico-Biological Interactions*, 2012, **199**, 192–200.
760 https://doi.org/10.1016/j.cbi.2012.08.013.
761 57 X. Wang, D. Li, L. Fan, Q. Xiao, H. Zuo and Z. Li, CAPE-pNO2 ameliorated diabetic
762 nephropathy through regulating the Akt/NF-κB/ iNOS pathway in STZ-induced diabetic
763 mice, *Oncotarget*, 2017, **8**, 114506–114525. https://doi.org/10.18632/oncotarget.23016.
764 58 W. S. Yang, D. Jeong, Y. S. Yi, J. G. Park, H. Seo, S. H. Moh, S. Hong and J. Y. Cho,
765 IRAK1/4-targeted anti-inflammatory action of caffeic acid, *Mediators of Inflammation*, ,
766 DOI:10.1155/2013/518183. https://doi.org/10.1155/2013/518183.
767 59 V. Sorrenti, M. Raffaele, L. Vanella, R. Acquaviva, L. Salerno, V. Pittalà, S. Intagliata
768 and C. Di Giacomo, Protective effects of caffeic acid phenethyl ester (Cape) and novel
769 cape analogue as inducers of heme oxygenase-1 in streptozotocin-induced type 1
770 diabetic rats, *International Journal of Molecular Sciences*, 2019, **20**, 1–13.
771 https://doi.org/10.3390/ijms20102441.
772 60 C. T. Capaldo and A. Nusrat, Cytokine regulation of tight junctions, *Biochimica et*
773 *Biophysica Acta*, 2009, **1788**, 864–871. https://doi.org/10.1016/j.bbamem.2008.08.027.
774 61 L. Tong, V. Tergaonkar, B. Key and C. Regulators, Rho protein GTPases and their
775 interactions with NF κ B : crossroads of inflammation and matrix biology,2014, 283–
776 295. https://doi.org/10.1042/BSR20140021.

777 62 W. Pan, H. Yu, S. Huang and P. Zhu, Resveratrol Protects against TNF- α -Induced
778 Injury in Human Umbilical Endothelial Cells through Promoting Sirtuin-1-Induced
779 Repression of NF-KB and p38 MAPK, *PLoS ONE*, 2016, **11**, 1–21.
780 https://doi.org/10.1371/journal.pone.0147034.
781 63 D. de Sá Coutinho, M. T. Pacheco, R. L. Frozza and A. Bernardi, Anti-Inflammatory
782 Effects of Resveratrol : Mechanistic Insights, *International Journal of Molecular*
783 *Sciences*, 2018, **19**, 1–25. https://doi.org/10.3390/ijms19061812.
784 64 C. Cerutti and A. J. Ridley, Endothelial cell-cell adhesion and signaling, *Experimental*
785 *Cell Research*, 2017, **358**, 31–38. https://doi.org/10.1016/j.yexcr.2017.06.003.
786 65 I. Chrobak, S. Lenna, L. Stawski and M. Trojanowska, Interferon-γ Promotes Vascular
787 Remodeling in Human Microvascular Endothelial Cells by Upregulating Endothelin
788 (ET)-1 and Transforming Growth Factor (TGF) β2, *Journal of celllular physiology*,
789 2014, **228**, 1774–1783. https://doi.org/10.1002/jcp.24337.Interferon-.
790 66 A. J. Minagar A, Long A, Ma T, Jackson TH, Kelley RE, Ostanin DV, Sasaki M, Warren
791 AC, Jawahar A, Cappell B, Interferon (IFN)-beta 1a and IFN- beta 1b block IFN-
792 gamma-induced disintegration of endothelial junction integrity and barrier, *Endothelium*,
793 2003, **10**, 299–307.
794 67 H. Amawi, C. R. J. Ashby, T. Samuel, R. Peraman and amit K. Tiwari, Polyphenolic
795 Nutrients in Cancer Chemoprevention and Metastasis : Role of the Epithelial-to-
796 Mesenchymal (EMT) Pathway, *Nutrients*, 2017, **9**, 1–23.
797 https://doi.org/10.3390/nu9080911.
798 68 Y. Yang, Y. Li, K. Wang, Y. Wang, W. Yin and L. Li, P38 / NF- k B / Snail Pathway Is
799 Involved in Caffeic Acid- Induced Inhibition of Cancer Stem Cells-Like Properties and
800 Migratory Capacity in Malignant Human Keratinocyte,2013, **8**, 1–8.
801 https://doi.org/10.1371/journal.pone.0058915.
802 69 X. Cheng, S. He, J. Yuan, S. Miao, H. Gao, J. Zhang, Y. Li, W. Peng and P. Wu,
803 Lipoxin A4 attenuates LPS-induced mouse acute lung injury via Nrf2-mediated E-

804 cadherin expression in airway epithelial cells, *Free Radical Biology and Medicine*, 2016,
805 **93**, 52–66. https://doi.org/10.1016/j.freeradbiomed.2016.01.026.
806
807
808
809
810
811
812
813
814
815
816
817
818
819
820
821
822
823
824
825
826
827
828
829
830

831 **Tables**

832

833 **Table 1.** Characterization of the phenolic composition of both red (rWPP) and white (wWPP)
834 wine pomace product digested fractions by GC-MS/MS and HPLC/DAD.
835

	Content (µg/g rWPP)		Content (µg/g wWPP)	
	rWPGI	rWPF	wWPGI	wWPF
TOTAL PHENOLIC ACIDS	**201 ± 16[a]**	**275 ± 42[b]**	**289 ± 16[b]**	**311 ± 28[b]**
Hydroxybenzoic acids	*159 ± 11[a]*	*186 ± 27[ab]*	*154 ± 8[a]*	*218 ± 6[b]*
Hydroxycinnamic acids	*42.2 ± 5.8[a]*	*89.1 ± 15.8[b]*	*135 ± 8[c]*	*92.6 ± 24.8[b]*
TOTAL STILBENS	**0.9 ± 0.1[a]**	**1.5 ± 0.1[c]**	**2.26 ± 0.02[d]**	**0.75 ± 0.07[a]**
TOTAL FLAVAN-3-OLS	**226 ± 7[b]**	**333 ± 33[c]**	**166 ± 14[a]**	**295 ± 24[c]**
Flavan-3-ols (monomers)	*180 ± 7[c]*	*195 ± 30[c]*	*32.2 ± 5.4[a]*	*75.6 ± 8.4[b]*
Flavan-3-ols (dimers)	*45.9 ± 0.1[a]*	*138 ± 9[b]*	*134 ± 10[b]*	*219 ± 15c*
TOTAL FLAVONOLS	**121 ± 10[c]**	**12.5 ± 0.1[a]**	**125 ± 15c**	**54.1 ± 1.1[b]**

836
837 [1] Content expressed as mean values ± standard deviation (n=3).
838 [2] Letters indicate significant differences (p<0,05) between samples for each phenolic compound
839 group (ANOVA, $p < 0.05$).
840 [3] rWPGI, potentially bioavailable gastrointestinal digestion fraction of the red wine pomace
841 product; rWPF, potentially bioavailable colonic fermentation fraction of the red wine pomace
842 product; wWPGI, potentially bioavailable gastrointestinal digestion fraction of the white wine
843 pomace product; wWPP, potentially bioavailable colonic fermentation fraction of the white wine
844 pomace product.
845

846

847

848

849

850

851

852

853

854

855

856

857

858

859 **Figure captions**

860 **Figure 1. MTT assay to determine the cell viability of EA.hy926 endothelial cells grown**
861 **under either normoglycemic or hyperglycemic conditions and treated for 24 h with both red**
862 **(rWPP) and white (wWPP) wine pomace product-digested fractions.** Results are expressed
863 as mean values ± standard deviation (n=4). Significant differences ($p < 0.05$) between
864 normoglycemic and hyperglycemic cells are indicated with an asterisk (*). Significant differences
865 ($p<0.05$) between the control, the WPGI-, and the WPF-treated cells are expressed in Roman
866 (normoglycemic) and Greek letters (hyperglycemic).

867 **Figure 2. Real-time monitoring of wine pomace product digested fractions mediating cell**
868 **viability and proliferation.** 24 hours after seeding EA.hy926 endothelial cells were treated with
869 the digested fractions of red (rWPP) and white (wWPP) wine pomace products (2.5 µg GAE/ml)
870 and the Cell Index was continuously monitored over 120 hours. The cell index is an arbitrary unit
871 for recording impedance and represents cell status in an electrode-containing well. The figure
872 represents the growing curves under normoglycemic conditions for treatments with: **(a)** the
873 rWPP-digested fractions**; (b)** the wWPP-digested fractions; **(c)** the correspondent slope curves
874 calculated for the 30-75 hours interval; **(d)** the growing curves under hyperglycemic conditions
875 for the rWPP-digested fractions; **(e)** for the wWPP-digested fractions; and, **(f)** treatments and the
876 corresponding slope curves calculated for the 30-75 hour interval. Results are expressed as mean
877 values ± standard deviation (n=3). Significant differences ($p<0.05$) between the control, the
878 WPGI-, and the WPF-treated cells are expressed in Roman letters.

879 **Figure 3. NO and ROS production in normo- and hyper-glicemia in differentiated**
880 **endothelial Ea.hy926 monolayer. (a)** NOX4 expression. Values are expressed as 2-ΔΔCt
881 normalized to the normoglycemic control cells. **(b)** Intracellular ROS levels. Intracellular ROS
882 production was estimated by increases of 2,7-dichlorofluorescein (DCF) fluorescence with
883 respect to the DCF fluorescence of the normoglycemic control sample. **(c)** Extracellular NO
884 levels. NO generation was estimated as the concentration in the culture medium of all NO
885 breakdown products ($NO_2^- + NO_3^-$). Results are expressed as mean values ± standard deviation

886 (n=4). Significant differences ($p < 0.05$) between normoglycemic and hyperglycemic cells are
887 indicated with an asterisk (*). Significant differences ($p<0.05$) between the control, the WPGI-,
888 and the WPF-treated cells are expressed in Roman (normoglycemic) and Greek letters
889 (hyperglycemic).

890 **Figure 4. The protective effect of wine pomace products on endothelial barrier function**
891 **assessed by RTCA platform. (a)** Normalized cell index over time for the normoglycemic cells
892 treated with the rWPP- ***(I)*** and wWPP- ***(II)*** digested fractions and stimulated with interferon-γ
893 (INF-γ). The normalized cell index over time for the hyperglycemic cells treated with the rWPP-
894 ***(III)*** and wWPP- ***(IV)*** digested fractions and stimulated with interferon-γ (INF-γ) are also shown.
895 **(b)** The barrier function calculated as the maximal change in the cell index and expressed as a
896 percentage of the control sample (100%) for the normoglycemic ***(I)*** and hyperglycemic ***(II)*** cells
897 treated with the rWPP- and wWPP-digested fractions. Significant differences ($p<0.05$) between
898 the control, the WPGI-, and the WPF-treated cells are expressed in Roman letters.

899 **Figure 5. NO and ROS production in normo- and hyper-glycemia in presence of interferon.**
900 **(a)** NOX4 expression. Values are expressed as 2-ΔΔCt normalized to the normoglycemic control
901 cells. **(b)** Intracellular ROS levels. Intracellular ROS production was estimated by increases of
902 2,7-dichlorofluorescein (DCF) fluorescence with respect to the DCF fluorescence of the
903 normoglycemic control sample. **(c)** Extracellular NO levels. NO generation was estimated as the
904 concentration in the culture medium of all NO breakdown products ($NO_2^- + NO_3^-$). Results are
905 expressed as mean values ± standard deviation (n=4). Significant differences ($p < 0.05$) between
906 normoglycemic and hyperglycemic cells are indicated with an asterisk (*). Significant differences
907 ($p<0.05$) between the control, the WPGI-, and the WPF-treated cells are expressed in Roman
908 (normoglycemic) and Greek letters (hyperglycemic).

909 **Figure 6. Phase contrast microscopy and immunofluorescence staining of VE-cadherin (red)**
910 **and Phalloidin-F-actin (green) in EA.hy926 endothelial cells pre-treated for 4 h with the**
911 **rWPP and wWPP-digested fractions, followed either by stimulation with Interferon-gamma**
912 **(3000 U/ml) for 1.5 h or left untreated (Control) under either Normoglycemic or**

913 **Hyperglycemic conditions. (a)** Phase contrast microscopy of either untreated or INF-γ-treated
914 EA.hy926 cells under normo- or hyperglycemic conditions. **(b)** Immunofluorescence staining of
915 Phalloidin-F-actin (green), VE-cadherin (red) and nuclear-DAPI-staining (blue) of EA-hy926
916 cells under normo- or hyperglycemic conditions and treated with the rWPP and wWPP-digested
917 fractions. **(c)** Quantification of the cell-cell spaces area by ImageJ software analysis and expressed
918 as number of pixels under normoglycemic ***(I)*** and hyperglycemic ***(II)*** conditions. **(d)** E-cadherin
919 intensity assessed by ImageJ and expressed as number of pixels under normoglycemic ***(I)*** and
920 hyperglycemic ***(II)*** conditions. **(e)** E-cadherin gene expression showed as 2-ΔΔCt normalized to
921 the normoglycemic control cells. ***(I)*** and hyperglycemic ***(II)*** conditions. Normoglycemic Control:
922 normoglycemic EA.hy926 endothelial cells neither treated with the WPPs nor treated with
923 interferon-gamma stimulation. Hyperglycemic Control: hyperglycemic EA.hy926 endothelial
924 cells neither treated with the WPPs nor treated with interferon-gamma stimulation. INF-γ: control
925 EA.hy926 endothelial cells not treated with the WPPs and treated with interferon-gamma.
926 rWPGI+INF-γ: EA.hy926 endothelial cells treated with the potentially bioavailable
927 gastrointestinal digestion fraction of the red wine pomace product and stimulated with interferon-
928 gamma. rWPF+INF-γ: EA.hy926 endothelial cells treated with the potentially bioavailable
929 colonic fermentation fraction of the red wine pomace product and stimulated with interferon-
930 gamma. wWPGI+ INF-γ: EA.hy926 endothelial cells treated with the potentially bioavailable
931 gastrointestinal digestion fraction of the white wine pomace product and stimulated with
932 interferon-gamma. wWPF+ INF-γ: EA.hy926 endothelial cells treated with the potentially
933 bioavailable colonic fermentation fraction of the white wine pomace product and stimulated with
934 interferon-gamma.

Figure 1

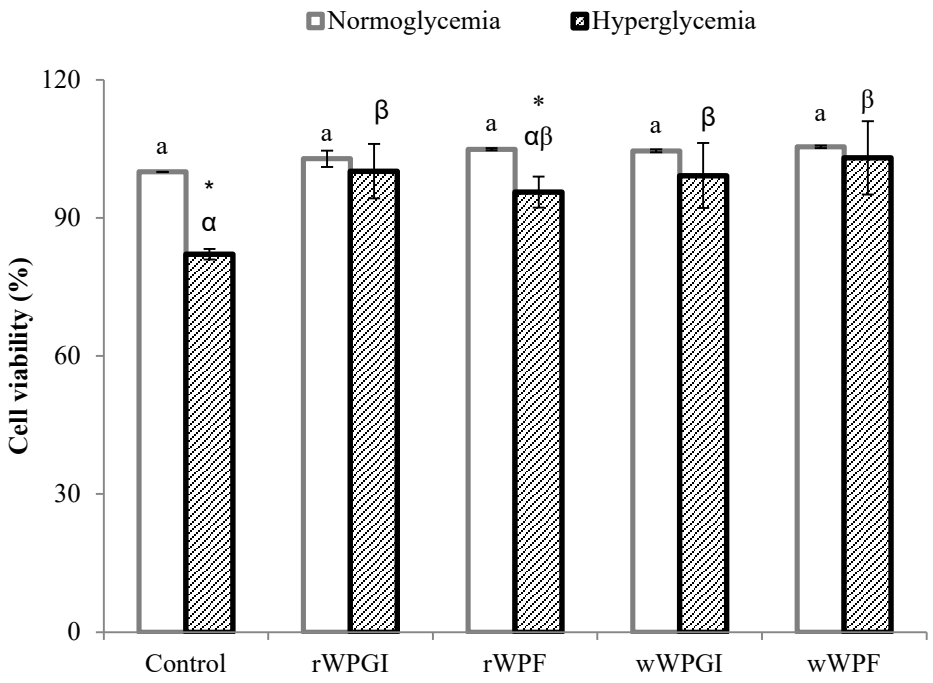
Normoglycemia
Hyperglycemia
Cell viability (%)
120
90
60
30
0
a
*
α
a
β
a
*
αβ
a
β
a
β
Control
rWPGI
rWPF
wWPGI
wWPF

Figure 2

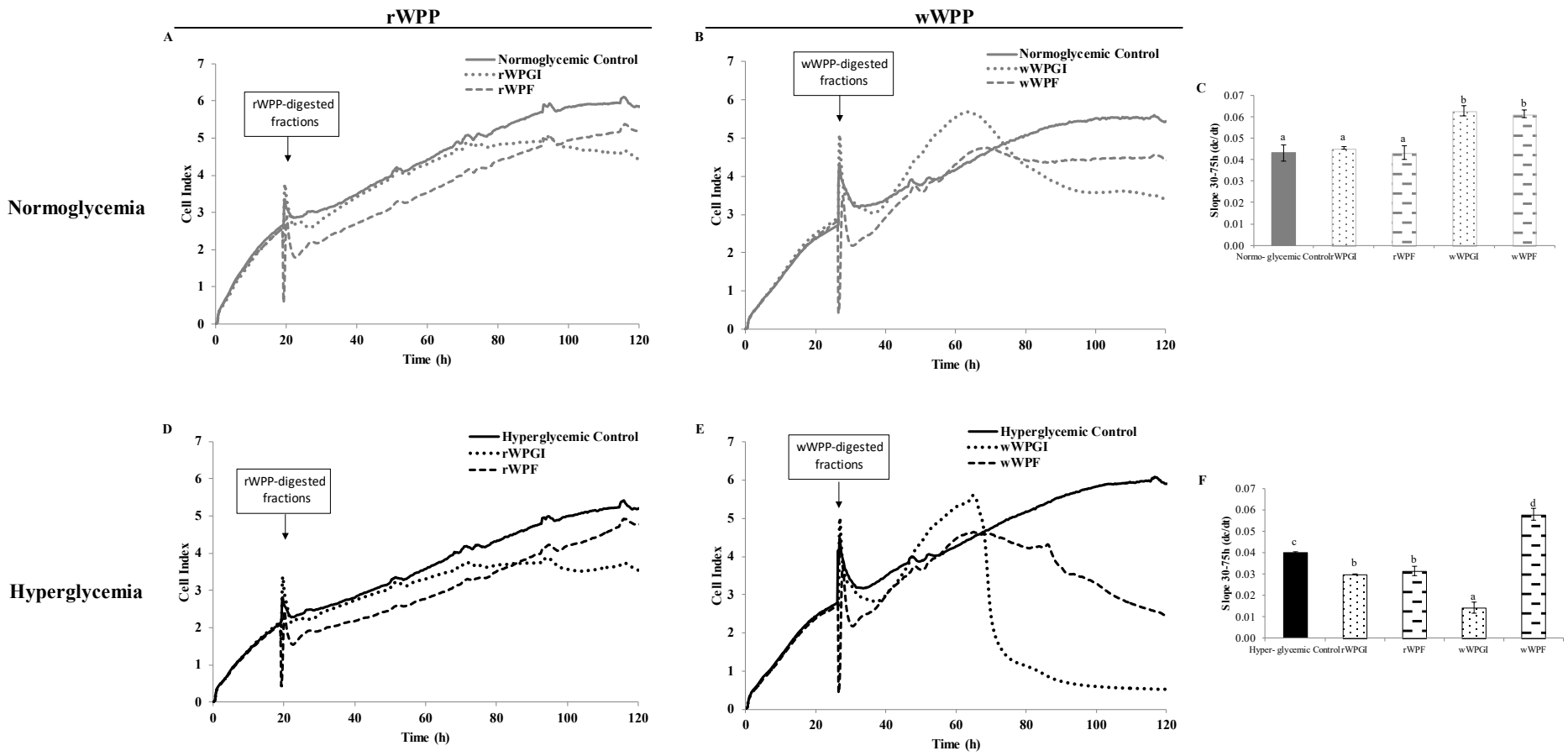
rWPP
wWPP
A
B
C
D
E
F
Normoglycemia
Hyperglycemia
rWPP-digested fractions
wWPP-digested fractions
Normoglycemic Control
rWPGI
rWPF
wWPGI
wWPF
Hyperglycemic Control
Cell Index
Time (h)
Slope 30-75h (dc/dt)
Normo- glycemic Control
Hyper- glycemic Control

Figure 3

A

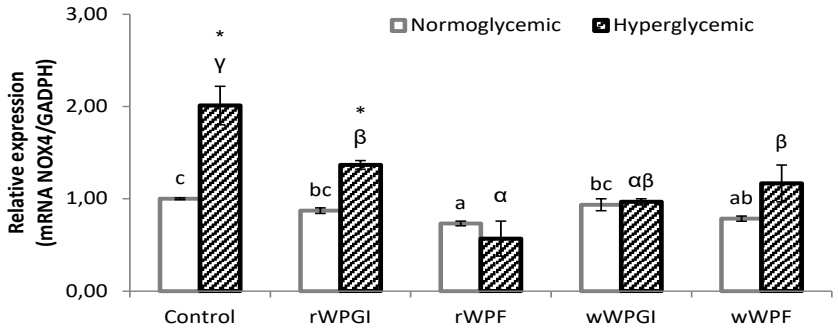
Normoglycemic
Hyperglycemic
Relative expression (mRNA NOX4/GADPH)
3,00
2,00
1,00
0,00
Control
rWPGI
rWPF
wWPGI
wWPF

B

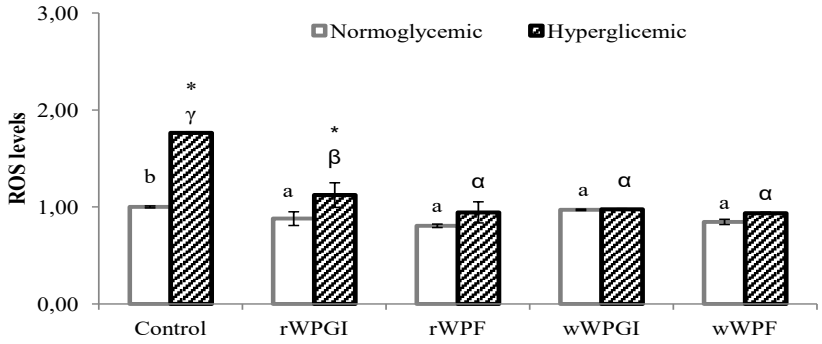
Normoglycemic
Hyperglicemic
ROS levels
3,00
2,00
1,00
0,00
Control
rWPGI
rWPF
wWPGI
wWPF

C

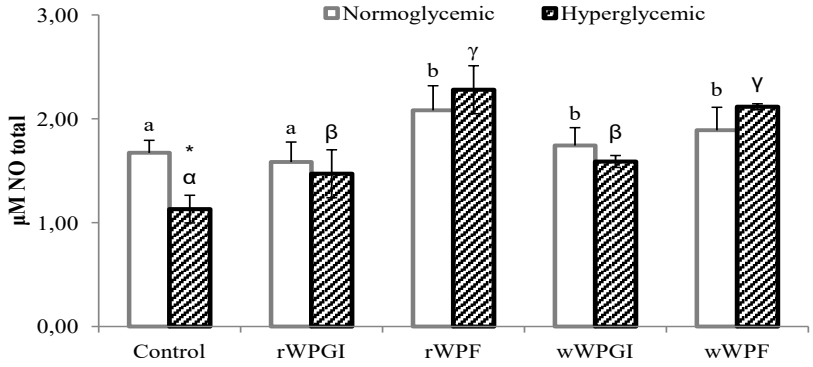
Normoglycemic
Hyperglycemic
µM NO total
3,00
2,00
1,00
0,00
Control
rWPGI
rWPF
wWPGI
wWPF

Figure 4

A

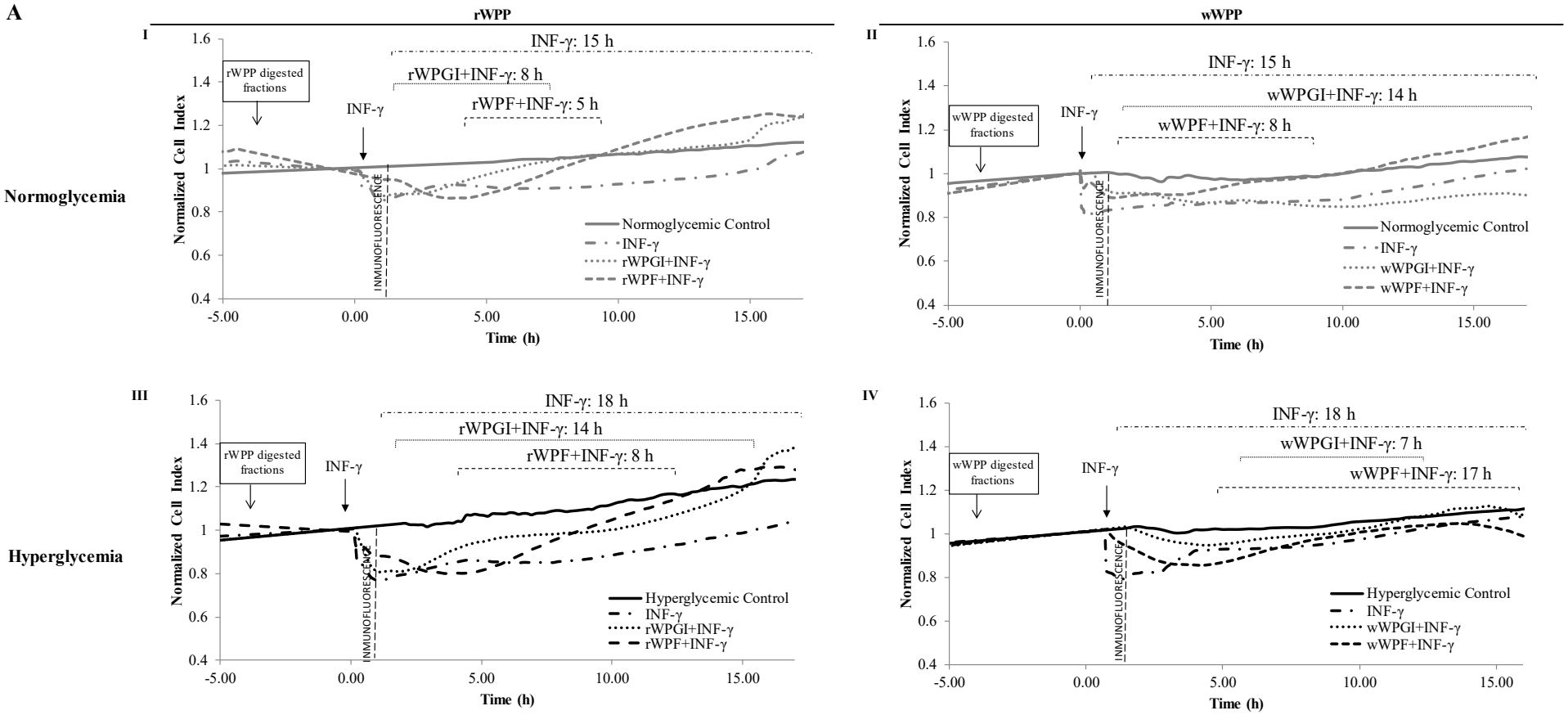
rWPP
wWPP
I
II
III
IV
Normoglycemia
Hyperglycemia
rWPP digested fractions
wWPP digested fractions
INF-γ
INMUNOFLUORESCENCE
INF-γ: 15 h
rWPGI+INF-γ: 8 h
rWPF+INF-γ: 5 h
wWPGI+INF-γ: 14 h
wWPF+INF-γ: 8 h
INF-γ: 18 h
rWPGI+INF-γ: 14 h
rWPF+INF-γ: 8 h
wWPGI+INF-γ: 7 h
wWPF+INF-γ: 17 h
Normalized Cell Index
Time (h)
Normoglycemic Control
Hyperglycemic Control
INF-γ
rWPGI+INF-γ
rWPF+INF-γ
wWPGI+INF-γ
wWPF+INF-γ

B

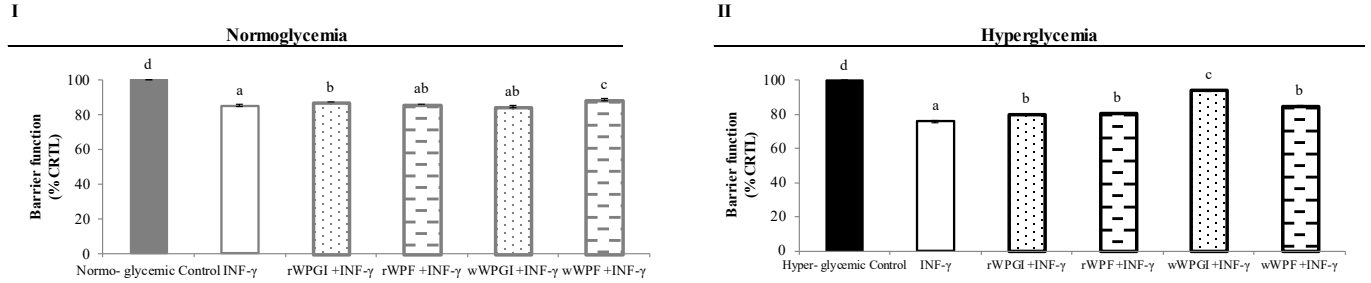
I
II
Normoglycemia
Hyperglycemia
Barrier function (% CRTL)
Normo- glycemic Control
Hyper- glycemic Control
INF-γ
rWPGI +INF-γ
rWPF +INF-γ
wWPGI +INF-γ
wWPF +INF-γ

Figure 5

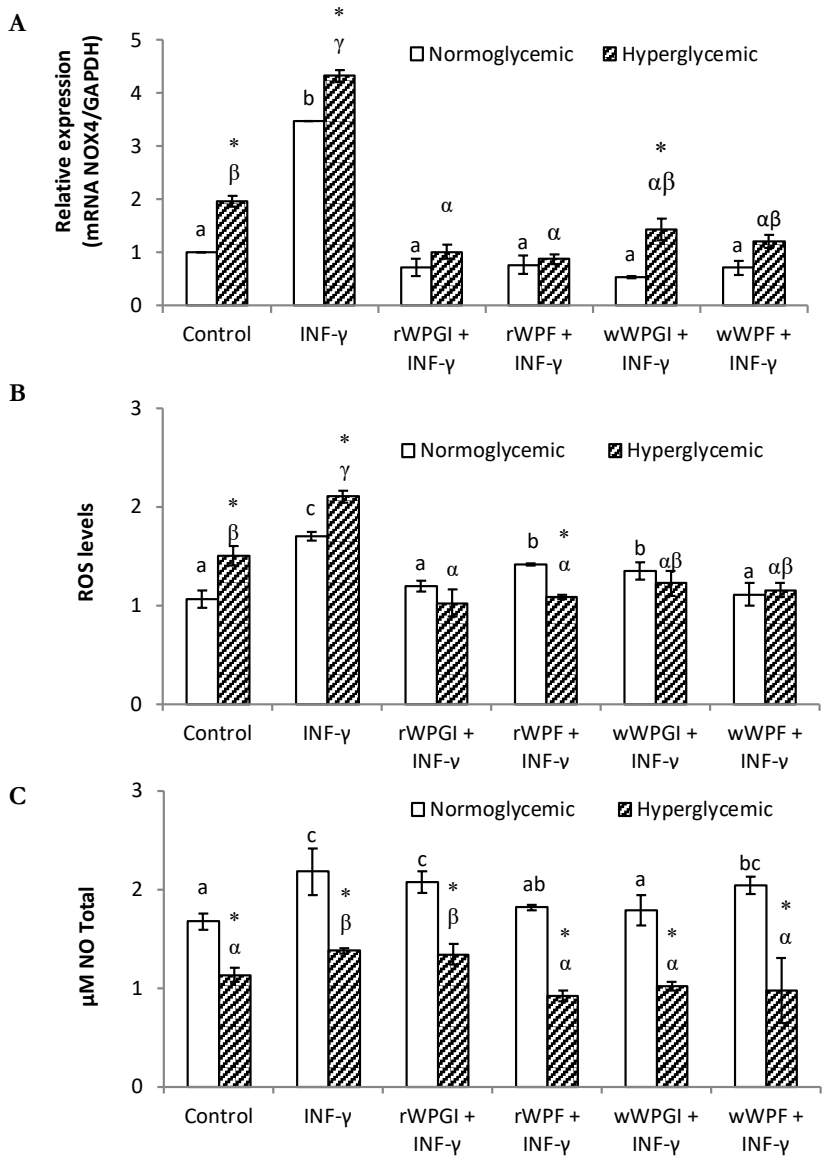
A
Relative expression (mRNA NOX4/GAPDH)
Normoglycemic
Hyperglycemic
Control
INF-γ
rWPGI + INF-γ
rWPF + INF-γ
wWPGI + INF-γ
wWPF + INF-γ
B
ROS levels
Normoglycemic
Hyperglycemic
Control
INF-γ
rWPGI + INF-γ
rWPF + INF-γ
wWPGI + INF-γ
wWPF + INF-γ
C
µM NO Total
Normoglycemic
Hyperglycemic
Control
INF-γ
rWPGI + INF-γ
rWPF + INF-γ
wWPGI + INF-γ
wWPF + INF-γ

Figure 6

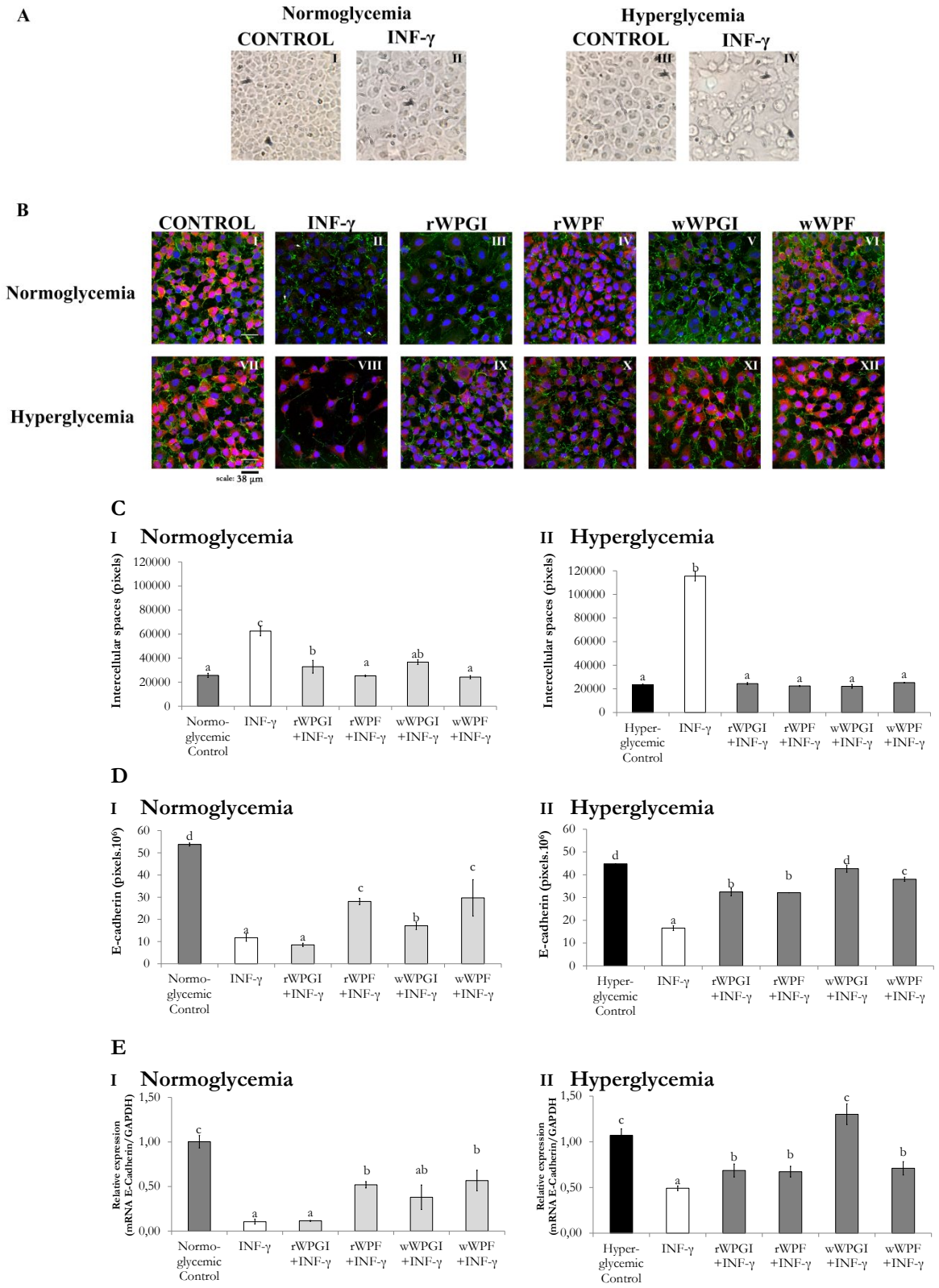
A
Normoglycemia
CONTROL
INF-γ
Hyperglycemia
CONTROL
INF-γ
B
CONTROL
INF-γ
rWPGI
rWPF
wWPGI
wWPF
Normoglycemia
Hyperglycemia
scale: 38 µm
C
I Normoglycemia
II Hyperglycemia
Intercellular spaces (pixels)
Normo-glycemic Control
Hyper-glycemic Control
INF-γ
rWPGI +INF-γ
rWPF +INF-γ
wWPGI +INF-γ
wWPF +INF-γ
D
I Normoglycemia
II Hyperglycemia
E-cadherin (pixels.10⁶)
E
I Normoglycemia
II Hyperglycemia
Relative expression (mRNA E-Cadherin/GAPDH)